Organometallic Clusters

DOI: 10.1002/ange.201407997

A Carbene-Rich but Carbonyl-Poor $[Ir_6(IMe)_8(CO)_2H_{14}]^{2+}$ Polyhydride Cluster as a Deactivation Product from Catalytic Glycerol Dehydrogenation**

Jesús Campos, Liam S. Sharninghausen, Robert H. Crabtree,* and David Balcells**

Abstract: *The title cluster, a deactivation product in the catalytic dehydrogenation of glycerol, was characterized by XRD, DFT calculations, HRMS, FTIR spectroscopy, and NMR spectroscopy. Experimental/computational studies located the 14 H ligands, and all ^1H and $^{13}C\{^1H\}$ NMR resonances were assigned. The structure contains an unprecedented Ir_6H_{14} core with two CO and eight IMe ligands.*

Low-valent metal clusters are dominated by metal carbonyl clusters. Clusters with few CO ligands are much rarer. Catalyst deactivation can form new clusters, whose structures can suggest preventive measures.[1–3] Our previously reported H-transfer catalyst,[4] $[Ir(cod)(IMe)_2]BF_4$ (**1**; IMe = 1,3-dimethylimidazol-2-ylidene), catalyzes glycerol conversion into lactic acid [Eq. (1)].[5] The title cluster, a deactivation product in Equation (1) and formed without external H_2, has an unusual structure, which was assigned computationally.

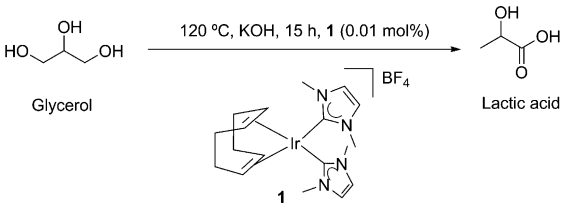

(1)

The hydride region of the ^1H NMR spectra obtained after the deactivation of **1** was complicated.[5] After 40 h at 120 °C in glycerol/H_2O (1:1) with KOH (30 equiv with respect to **1**), complex **2** was isolated. Only BAr_F ($BAr_F = B\{3,5\text{-}C_6H_3(CF_3)_2\}_4^-$) gave suitable crystals of cluster **2** (Figure 1) after extraction with CH_2Cl_2, concentration, and layering with pentane at −20 °C for 24 h.

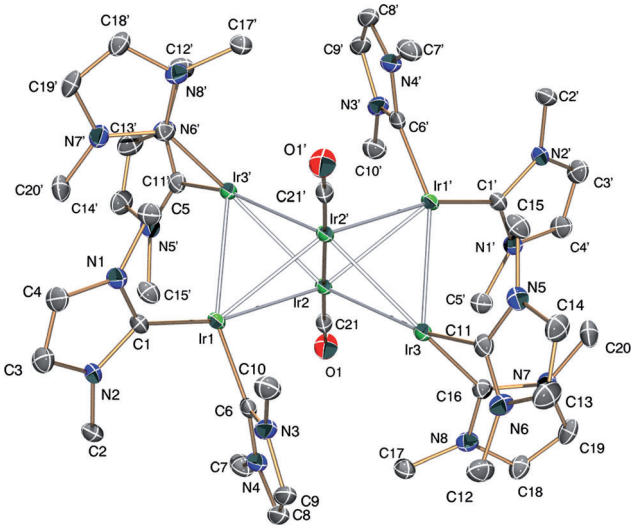

Figure 1. ORTEP diagram of the cationic portion of compound **2**. Thermal ellipsoids are shown at 50%. Hydrogen atoms, two BAr_F counterions, and a pentane solvent molecule have been omitted for clarity. The metal hydrides were not located in the Fourier map.

Complex **2** contains two Ir(CO) groups, which give rise to FTIR bands at 1950 and 1965 cm^{-1}. These CO ligands must come from the decarbonylation of glyceraldehyde. The geometry of **2** is a "bow tie" or edge-sharing bitetrahedron,[6] previously unreported for Ir complexes, other than in a Au–Ir cluster.[7] In spite of its high-temperature formation,[8] it retains 14 H ligands (according to ^1H NMR spectroscopic data and DFT calculations). The hydride content was confirmed by high-resolution MS (FTICR; Figure 2): {m/z = 996.2123 (z = +2)} had the expected isotopic distribution and exhibited a continuous mass increment of 0.5 consistent with an overall charge of +2. The high N-heterocyclic-carbene (NHC) content is surprising, since reductive elimination of the imidazolium salt might have been expected.[9–11] Previously reported Ru and Os clusters typically have only 1–2 NHC ligands per cluster;[12–14] attempts to incorporate more than two such ligands failed.[14a,15,16] Cluster formation from mononuclear metal–NHC precursors is unknown, but this cluster contains a record number of NHC ligands. The unhindered NHC ligand, with only NMe groups, probably facilitates the binding of multiple ligands.

[*] J. Campos, L. S. Sharninghausen, Prof. R. H. Crabtree
Department of Chemistry, Yale University
225 Prospect Street, New Haven, Connecticut 06520 (USA)
E-mail: jesus.camposmanzano@yale.edu
robert.crabtree@yale.edu
Dr. D. Balcells
Department of Chemistry, University of Oslo, Centre of Excellence in Theoretical and Computational Chemistry (CTCC)
N-0315 Oslo (Norway)
E-mail: david.balcells@kjemi.uio.no

[**] This research was supported by the CCHF, an EFRC funded by the US DoE, Office of Science, Office of Basic Energy Sciences, under DE-SC0001298 (R.H.C. and J.C., synthesis), and by their catalysis award (L.S.S., J.C., DE-FG02-84ER13297, characterization). D.B. acknowledges support from the Norwegian Research Council through the Center of Excellence for Theoretical and Computational Chemistry (CTCC; Grant No. 179568V30) and the Norwegian Metacenter for Computational Science (NOTUR; Grant nn4654k). D.B. also thanks the EU REA for a Marie Curie Fellowship (Grant CompuWOC/618303).

Supporting information for this article is available on the WWW under http://dx.doi.org/10.1002/anie.201407997.

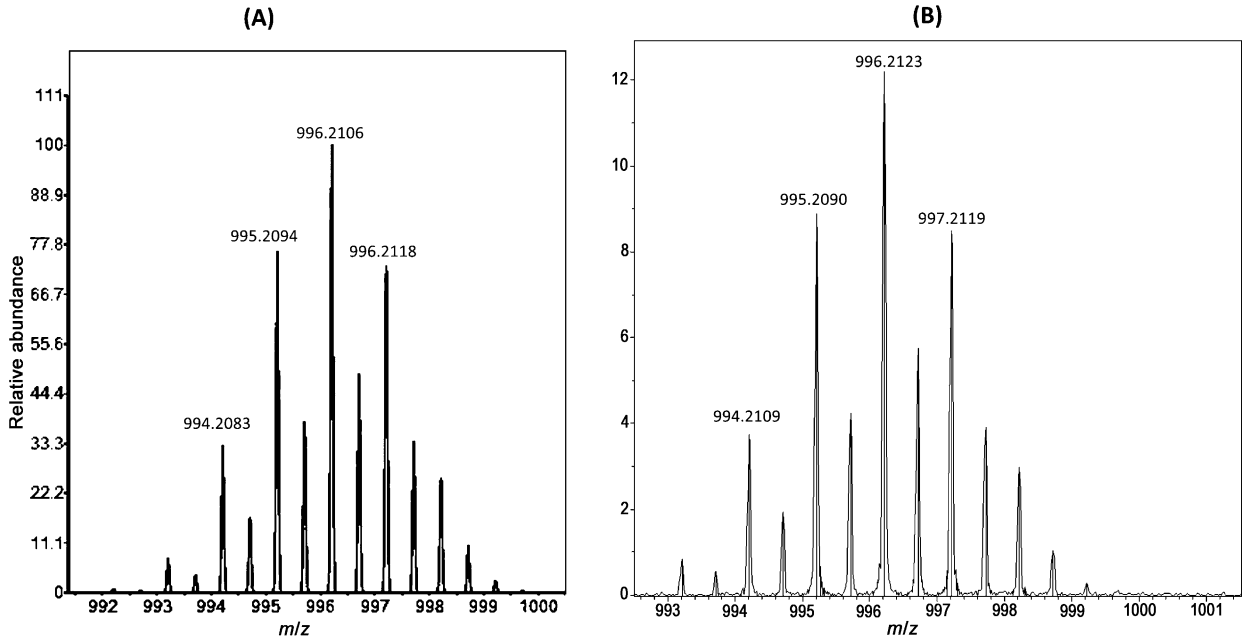

Figure 2. A) Experimental and B) calculated HRMS (FTICR) spectra of cation **2** ($[Ir_6(IMe)_8(CO)_2H_{14}]^{2+}$).

Originally, NMR spectroscopic data for **2** was unavailable because of its low yield (< 1 %; see Table S1 in the Supporting Information), but its formation was enhanced by combining [Ir(IMe)(cod)Cl] or [{Ir(cod)(μ-Cl)}$_2$] with [Ir(cod)-(IMe)$_2$]BF_4. Weller and co-workers described a similar cluster synthesis from "naked" Rh and a Rh precursor.[17] Screening (see Table S1) identified the best reaction conditions for the formation of **2**: The use of [Ir(IMe)(cod)Cl] raised the yield of **2** to approximately 12 %, with **2** and [Ir(IMe)(cod)Cl] present in a 1:1 ratio.

^{1}H and ^{13}C{^{1}H} NMR spectroscopic data for **2** showed 7 H resonances between −16 and −20 ppm; these signals were assigned to 14 H ligands. T_1 relaxation data from 233 to 333 K gave T_1(min) = 300–380 ms (see Figure S12 in the Supporting Information) and thus pointed to all-classical hydride ligands.[18,19] These atoms could not be located by XRD, but only by DFT calculations[20,21] at the wB97xd/LANLTZ*,6-311G** level (see the Supporting Information). The wB97xd hybrid functional[22] gave the best results when benchmarked against other functionals with the XRD structure of a related Ir cluster[23] (see Figure S13 and Table S4). The H positions were guessed from simple "textbook" rules. Full geometry optimization converged to the structure in Figure 3, with 10 bridging and 4 terminal H ligands, fully consistent with the ^{1}H NMR spectra and XRD data: Maximum and average (RMSD) deviations were 0.024 and 0.011 Å (Table 1; see also Figure S19).

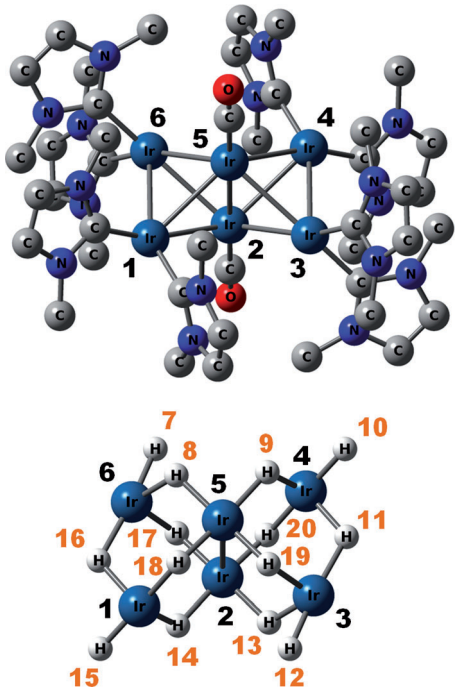

Figure 3. DFT-optimized geometry of **2** (top; hydrogen atoms removed for clarity) and its Ir_6H_{14} core (bottom).

The M–H distances are shorter for the terminal κ^1-H (1.583 and 1.589 Å) than for the bridging μ^2-H ligands (1.691–1.808 Å; see Table S5). The NBO6[24] natural charges on these H atoms (see Figure S14), range from −0.07 to −0.20. The μ^2-H ligands, 11 and 16 (Figure 3), link the four peripheral Ir^{III} units (1, 3, 4, and 6). The other 8 μ^2-H ligands connect the Ir–Ir σ-bonded Ir^{II} centers (2 and 5), consistent with the diamagnetism and the short Ir2–Ir5 distance (XRD: 2.691 Å, DFT: 2.695 Å). Furthermore, both the HOMO and the associated NBO contain an in-phase combination of the two metal d_{z^2} orbitals (see Figure S15). Noncovalent ligand-ligand and ligand-metal core interactions were mapped with the NCIPLOT approach (see Figure S16).[25,26] ^{1}H and ^{13}C 1D and 2D NMR spectroscopic analysis showed that the inversion center at the Ir–Ir σ bond of **2** is maintained in solution. Thus, the 8 NHC ligands give four sets of signals, whereas the

Table 1: Interatomic distances in **2** as determined by X-ray diffraction and DFT calculations.[a]

	X-ray diffraction	DFT (wB97xd)
Ir1–Ir3[b,c]	4.2595(6)	4.262
Ir1–Ir6[b,d]	3.0019(3)	3.001
Ir2–Ir5[b]	2.6908(5)	2.695
Ir1–Ir2[b,e]	2.9296(3)	2.935
Ir2–Ir3[b,f]	2.9426(4)	2.939
Ir2–Ir4[b,g]	2.9492(3)	2.946
Ir2–Ir6[b,h]	2.9076(4)	2.915
Ir1–C[b,i]	2.007(6)	2.027
Ir1–C′[b,j]	2.010(6)	2.027
Ir3–C[b,k]	2.014(6)	2.013
Ir3–C′[b,l]	2.043(6)	2.019
RMSD[m]		0.011
maximum deviation[n]		0.024

[a] See Figure 3 for atom labels. [b] Interatomic distances in Å. [c] Ir1–Ir3 = Ir4–Ir6. [d] Ir1–Ir6 = Ir3–Ir4. [e] Ir1–Ir2 = Ir4–Ir5. [f] Ir2–Ir3 = Ir5–Ir6. [g] Ir2–Ir4 = Ir1–Ir5. [h] Ir2–Ir6 = Ir3–Ir5. [i] Ir1–C = Ir4–C. [j] Ir1–C′ = Ir4–C′. [k] Ir3–C = Ir6–C. [l] Ir3–C′ = Ir6–C′. [m] Root-mean-square deviation in Å. [n] The maximum deviation is given in Å.

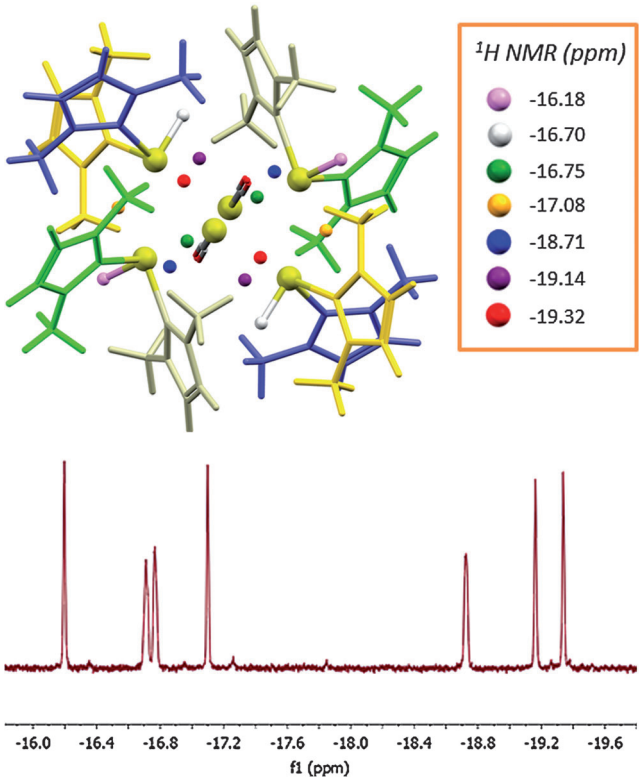

Figure 5. ^{1}H NMR hydride resonances and their color-coded assignment.

14 H ligands give seven signals (see the Supporting Information). First, the ^{1}H and ^{13}C{^{1}H} NMR signals due to the NHC ligands were separated into four groups on the basis of 2D HSQC, HMBC, and NOESY data (see Figure S6). In each group, we observed two aromatic NHC ^{1}H NMR peaks between 6.4 and 7.1 ppm (d, $^3J_{HH} \approx 2$ Hz), with ^{13}C{^{1}H} signals between 119 and 122 ppm. Two NMe singlets between 2.5 and 4.0 ppm were observed for each pair of equivalent NHC ligands, with corresponding ^{13}C{^{1}H} resonances at 38–46 ppm, thus highlighting the hindered rotation around the Ir–C bonds. ^{13}C{^{1}H} resonances at approximately 150 ppm were assigned to four independent carbene carbon atoms. NOE cross-peaks were traced for the seven MH resonances. M–H/NMe interactions gave 18 intense and 7 weaker NOE signals (Figure 4). The concordant XRD and DFT structures (Table 1) rationalized the NOESY spectrum on the basis of the DFT H···H distances between MH and NMe hydrogen atoms. Only one of the possible assignments was consistent with all the 2D NMR and DFT data (see the Supporting Information). We could then unequivocally assign all ^{1}H and ^{13}C{^{1}H} NMR resonances, including those of the 14 H ligands (Figure 5). As far as we are aware, the full assignment of the NMR spectroscopic data for such a big cluster has not been possible previously without a theoretical simulation.

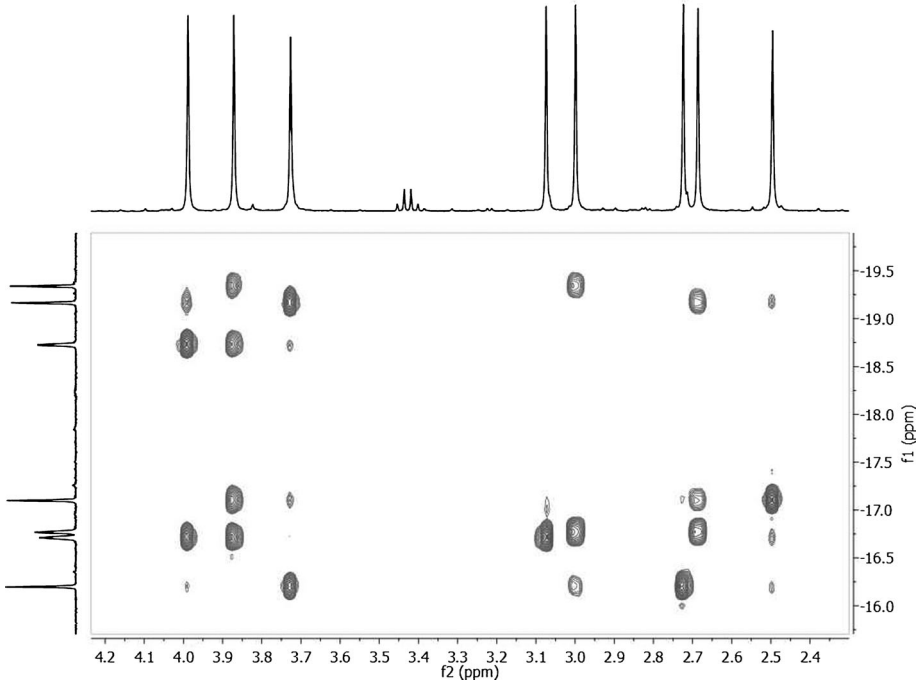

Figure 4. Selected region of the 2D NOESY spectrum of **2** exhibiting the interaction between the metal hydrides (*y* axis) and methyl wingtips (*x* axis).

The 2D EXSY NMR spectrum of **2** (see Figure S11) showed that one pair of NHC ligands (blue in Figure 5) can rotate in spite of the bulky ligand sphere (Figure 6) with

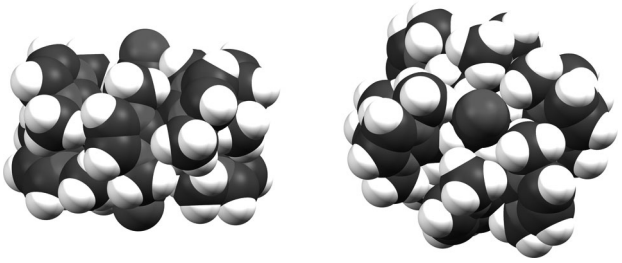

Figure 6. Space-filling representations of **2** ($[Ir_6(IMe)_8(CO)_2H_{14}]^{2+}$).

a rate constant of $0.93\,s^{-1}$ (25 °C) and $\Delta G^{\neq}_{298K} = 17.5 \pm 0.5\,kcal\,mol^{-1}$, in agreement with the DFT(wB97xd) barrier of $19.0\,kcal\,mol^{-1}$ for rotation by 60° (see Figure S18). As expected, no H/D isotopic exchange occurred in the presence of CD_3OD or D_2 even after several days at 50 °C.

In summary, a new Ir_6 cluster was formed in the catalytic conversion of glycerol into lactic acid. Prior iridium hydride clusters have been formed with H_2, but in this case we can omit H_2 because the H atoms come from glycerol. The structure of **2** is also significant because it: 1) is the first Ir_6 polyhydride; 2) is the first "bow-tie" all-Ir structure; 3) is the first high-nuclearity Ir compound with NHC ligands; 4) is the only metal cluster with more than two NHC ligands, and establishes a new synthesis of NHC-rich metal clusters, whose properties remain to be established.

Received: August 6, 2014
Published online: September 22, 2014

Keywords: deactivation · fluxionality · N-heterocyclic carbenes · NMR spectroscopy · nuclear Overhauser effect

[1] See, for example: a) C. P. Lenges, P. S. White, M. Brookhart, *J. Am. Chem. Soc.* **1998**, *120*, 6965 – 6979; b) C. S. Letko, Z. M. Heiden, T. B. Rauchfuss, *Eur. J. Inorg. Chem.* **2009**, 4927 – 4930; c) R. H. Crabtree, *Acc. Chem. Res.* **1979**, *12*, 331 – 338; d) S. P. Smidt, A. Pfaltz, E. Martínez-Viviente, P. S. Pregosin, A. Albinati, *Organometallics* **2003**, *22*, 1000 – 1009; A. Rifat, N. J. Patmore, M. F. Mahon, A. S. Weller, *Organometallics* **2002**, *21*, 2856 – 2865.

[2] For reviews, see: a) P. J. Dyson, J. S. McIndoe, *Angew. Chem. Int. Ed.* **2004**, *43*, 6028 – 6030; *Angew. Chem.* **2004**, *116*, 6152 – 6154; b) P. J. Dyson, J. S. McIndoe, *Angew. Chem. Int. Ed.* **2005**, *44*, 5772 – 5774; *Angew. Chem.* **2005**, *117*, 5918 – 5921; c) G. Lavigne, *Angew. Chem. Int. Ed.* **2012**, *51*, 5794 – 5796; *Angew. Chem.* **2012**, *124*, 5894 – 5896; d) G. Hogarth, S. E. Kabir, E. Nordlander, *Dalton Trans.* **2010**, *39*, 6153 – 6174.

[3] *Metal Clusters in Chemistry* (Eds.: P. Braunstein, L. A. Oro, P. R. Raithby), Wiley, New York, **1999**.

[4] a) J. Campos, U. Hintermair, T. P. Brewster, M. K. Takase, R. H. Crabtree, *ACS Catal.* **2014**, *4*, 973 – 985; b) U. Hintermair, J. Campos, T. P. Brewster, L. M. Pratt, N. D. Schley, R. H. Crabtree, *ACS Catal.* **2014**, *4*, 99 – 108.

[5] L. S. Sharninghausen, J. Campos, M. G. Manas, R. H. Crabtree, *Nat. Commun.* **2014**, *5*, DOI: 10.1038/ncomms6084.

[6] C. E. Briant, K. P. Hall, D. M. P. Mingos, A. C. Wheeler, *J. Chem. Soc. Dalton Trans.* **1986**, 687 – 692.

[7] R. D. Adams, M. Chen, X. Yang, *Organometallics* **2012**, *31*, 3588 – 3598.

[8] For examples of hydride-rich metal clusters, see: a) A. S. Weller, J. S. McIndoe, *Eur. J. Inorg. Chem.* **2007**, 4411 – 4423; b) R. F. Adams, B. Captain, *Angew. Chem. Int. Ed.* **2005**, *44*, 2531 – 2533; *Angew. Chem.* **2005**, *117*, 2587 – 2589; c) R. D. Adams, B. Captain, L. Zhu, *J. Am. Chem. Soc.* **2007**, *129*, 2454 – 2455; d) S. K. Brayshaw, M. J. Ingleson, J. C. Green, J. S. McIndoe, P. R. Raithby, G. Kociok-Kohn, A. S. Weller, *J. Am. Chem. Soc.* **2006**, *128*, 6247 – 6263; e) S. K. Brayshaw, A. Harrison, J. S. McIndoe, F. Marken, P. R. Raithby, J. E. Warren, A. S. Weller, *J. Am. Chem. Soc.* **2007**, *129*, 1793 – 1804; f) X. Li, J. Baldamus, M. Nishiura, O. Tardif, Z. Hou, *Angew. Chem. Int. Ed.* **2006**, *45*, 8184 – 8188; *Angew. Chem.* **2006**, *118*, 8364 – 8368; g) Y. Nakajima, S. Sakaki, Y. Nakao, H. Suzuki, *Organometallics* **2012**, *31*, 5342 – 5348.

[9] D. S. McGuinness, K. J. Cavell, *Organometallics* **2000**, *19*, 4918 – 4920.

[10] D. Bacciu, K. J. Cavell, I. A. Fallis, L.-I. Ooi, *Angew. Chem. Int. Ed.* **2005**, *44*, 5282 – 5284; *Angew. Chem.* **2005**, *117*, 5416 – 5418.

[11] C. M. Crudden, D. P. Allen, *Coord. Chem. Rev.* **2004**, *248*, 2247 – 2273.

[12] J. A. Cabeza, P. García-Álvarez, *Chem. Soc. Rev.* **2011**, *40*, 5389 – 5405.

[13] a) J. A. Cabeza, M. Damonte, P. García, M. G. Herna, A. R. Kennedy, *Organometallics* **2012**, *31*, 327 – 334; b) J. A. Cabeza, M. Damonte, P. García-Álvarez, E. Pérez-Carreño, *Organometallics* **2013**, *32*, 9251 – 9260.

[14] a) M. R. Crittall, C. E. Ellul, M. F. Mahon, O. Saker, M. K. Whittlesey, *Dalton Trans.* **2008**, 4209 – 4211; b) M. I. Bruce, M. L. Cole, R. S. C. Fung, C. M. Forsyth, M. Hilder, P. C. Junk, K. Konstas, *Dalton Trans.* **2008**, 4118 – 4128; c) C. Zhang, B. Li, H. Song, S. Xu, B. Wang, *Organometallics* **2011**, *30*, 3029 – 3036; d) Y. Liu, R. Ganguly, H. V. Huynh, W. K. Leong, *Angew. Chem. Int. Ed.* **2013**, *52*, 12110 – 12113; *Angew. Chem.* **2013**, *125*, 12332 – 12335.

[15] S. Warratz, L. Postigo, B. Royo, *Organometallics* **2013**, *32*, 893 – 897.

[16] J. A. Cabeza, M. Damonte, P. García-Álvarez, A. R. Kennedy, E. Pérez-Carreño, *Organometallics* **2011**, *30*, 826 – 833.

[17] S. K. Brayshaw, J. C. Green, R. Edge, E. R. L. McInnes, P. R. Raithby, J. E. Warren, A. S. Weller, *Angew. Chem. Int. Ed.* **2007**, *46*, 7844 – 7848; *Angew. Chem.* **2007**, *119*, 7990 – 7994.

[18] D. G. Hamilton, R. H. Crabtree, *J. Am. Chem. Soc.* **1988**, *110*, 4126 – 4133.

[19] W. J. Oldham, Jr., A. S. Hinkle, D. M. Heinekey, *J. Am. Chem. Soc.* **1997**, *119*, 11028 – 11036.

[20] S. K. Brayshaw, J. C. Green, N. Hazari, A. S. Weller, *Dalton Trans.* **2007**, 1781 – 1792.

[21] M. Plois, W. Hujo, S. Grimme, C. Schwickert, E. Bill, B. Bruin, R. Pöttgen, R. Wolf, *Angew. Chem. Int. Ed.* **2013**, *52*, 1314 – 1318; *Angew. Chem.* **2013**, *125*, 1352 – 1357.

[22] J.-D. Chai, M. Head-Gordon, *Phys. Chem. Chem. Phys.* **2008**, *10*, 6615 – 6620.

[23] Y. Xu, M. A. Celik, A. L. Thompson, H. Cai, M. Yurtsever, B. Odell, J. C. Green, D. M. P. Mingos, J. M. Brown, *Angew. Chem. Int. Ed.* **2009**, *48*, 582 – 585; *Angew. Chem.* **2009**, *121*, 590 – 593.

[24] E. D. Glendening, C. R. Landis, F. Weinhold, *J. Comput. Chem.* **2013**, *34*, 1429 – 1437.

[25] E. R. Johnson, S. Keinan, P. Mori-Sánchez, J. Contreras-García, A. J. Cohen, W. Yang, *J. Am. Chem. Soc.* **2010**, *132*, 6498 – 6506.

[26] J. Contreras-García, E. R. Johnson, S. Keinan, R. Chaudret, J.-P. Piquemal, D. N. Beratan, W. Yang, *J. Chem. Theory Comput.* **2011**, *7*, 625 – 632.

